Three-axis Attitude Control with Two Reaction Wheels and Magnetic Torquer Bars

Bryce A. Roberts[*], Jeffrey W. Kruk[†], Thomas B. Ake[‡], Tom S. Englar[§]
Johns Hopkins University, Baltimore, MD 21210, USA

and

Brian F. Class[**], Daniel M. Rovner[††]
Orbital Sciences Corporation, Dulles, VA 20166 USA

The Far Ultraviolet Spectroscopic Explorer satellite was launched in 1999 and began a three-year prime mission to collect high-resolution spectra in the far ultraviolet bandpass. Two and a half years after launch, mechanical failure of two out of four reaction wheels reduced the satellite to two-axis control, halting science observations. This failure prompted modification of the FUSE attitude control system software to restore three-axis control using a hybrid of existing magnetic and reaction wheel actuators. Pointing accuracy and stability are once again at the sub-arcsecond level, close to the pre-wheel failure performance. The range of stable attitudes is limited, but ground-based modeling software now directs the planning process so that observations and maneuvers stay within the limits of the actuators. Despite these constraints, efficient science operations are ongoing, and over the course of a year, the entire sky is available for observation.

Nomenclature

$\vec{N}_{gg}$	=	gravity gradient torque
$GM_{\oplus}$	=	earth gravitational constant
$\vec{R}$	=	satellite earth-centered inertial (ECI) position vector
I	=	satellite inertia tensor
$\vec{\mu}$	=	spacecraft dipole moment vector
$\vec{B}$	=	geomagnetic field vector
$\vec{N}_{mag}$	=	magnetic torque vector
$\hat{S}$	=	"symmetric" body axis
$\hat{A}$	=	"anti-symmetric" (magnetic) body axis
k	=	unloading gain factor
θ_{error}	=	angular attitude error

[*] Mission Planner, Department of Physics and Astronomy, broberts@pha.jhu.edu, Member AIAA.
[†] Principal Research Scientist, Department of Physics and Astronomy
[‡] Head of Instrument Operations, also with Computer Sciences Corporation.
[§] Independent Consultant to FUSE Project.
[**] Senior Director, Attitude Control Systems Department, Senior Member AIAA.
[††] ACS Analyst, Attitude Control Systems Department.

I. Introduction

The Far Ultraviolet Spectroscopic Explorer (FUSE) was launched into low-earth orbit on 24 June 1999 and began a three-year prime mission to collect high-resolution astronomical spectra in the far ultraviolet bandpass[1]. The science instrument, a set of four co-aligned telescopes and prime focus spectrographs[2], is maneuvered by a spacecraft bus whose design evolved from previous Explorer Platform spacecraft. The Johns Hopkins University in Baltimore, Maryland is responsible for satellite command and control, and develops activity schedules on behalf of the international community of astronomers whose peer-reviewed programs have been granted observing time by NASA. Commands are uplinked by way of a ground station in Puerto Rico, and FUSE operates autonomously as it observes approximately 3-6 astronomical targets per day.

The science goals require that the satellite be able to achieve absolute pointing accuracy of ~1", maintain pointing stability of ~0.5", and autonomously slew between science targets in a fraction of one 100 minute long orbit. To accomplish this, the attitude control system (ACS) employs ring laser gyros and an optical fine error sensor for attitude knowledge, and reaction wheel assemblies (RWAs) to generate control torque. Three orthogonal RWAs control the yaw, pitch and roll body axes, and a fourth redundant skew wheel provides equal torque components along all three body axes. Each RWA can provide up to 55 m Nm of torque until the 21 Nms momentum storage limit is reached. Three orthogonal magnetic torquer bars (MTBs) with a maximum dipole moment of ~140 Am^2 act against the geomagnetic field to unload momentum from the RWAs and maintain a zero wheel momentum bias. Finally, tri-axial magnetometers (TAMs) measure the geomagnetic field in the body frame, and are used both for coarse two-axis attitude estimation as well as an input to the momentum unloading routine.

FUSE is in a circular orbit with an inclination of 25º and altitude of 765km. Aerodynamic drag torque at this altitude for a satellite of FUSE's size is negligible, so the only significant external disturbance is gravity gradient torque, given by

$$\vec{N}_{gg} = 3\frac{GM_{\oplus}}{\left\|\vec{R}\right\|^3}\hat{R}\times I\hat{R} \tag{1}$$

where $\vec{R}$ is the satellite's position vector relative to the center of the earth, $\hat{R}$ is the normalized unit direction vector version of $\vec{R}$ in the spacecraft body frame, and I is the spacecraft inertia tensor. The off-axis products in FUSE's inertia tensor are 1% of the diagonal terms, so Eq. 1 can be approximated by,

$$\vec{N}_{gg} \cong 3\frac{GM_{\oplus}}{\left\|\vec{R}\right\|^3}\begin{bmatrix} r_y r_z\left(I_{zz}-I_{yy}\right) \\ r_x r_z\left(I_{xx}-I_{zz}\right) \\ r_x r_y\left(I_{yy}-I_{xx}\right)\end{bmatrix} \tag{2}$$

where r_x, r_y, and r_z are the scalar components of $\hat{R}$. Inspection of Eq. (2) shows that gravity gradient torques are generally minimized when the spacecraft Z axis (the instrument boresight) is pointed perpendicular to the orbital plane, at which point r_z is 0. The magnitude of the gravity gradient torque increases as the boresight moves away from the orbit plane normal vector, reaching a maximum of ~5 m Nm; the components of this torque on each of the body axes depends on the attitude. There are four instantaneous gravity gradient torque minima when the boresight is pointed in the plane of the orbit.

The geomagnetic field can be accurately represented in the earth centered inertial (ECI) frame as a 10^{th} order expansion in spherical harmonics, for example the 1995 revision of the International Geomagnetic Reference Field (IGRF1995). Typical field strengths in FUSE's orbital environment vary between 1.7×10^{-5} and 4×10^{-5} T, and the field direction can also vary considerably as a function of orbital phase.

The torque generated as the MTBs act against the geomagnetic field, $\vec{N}_{mag} = \vec{\mu}\times\vec{B}$, is highly dependent on the alignment of $\vec{B}$ in the body frame, but given the 140 Am^2 dipole moment of three torquer bars, is typically in the range of 2 - 6 m Nm — approximately $1/10^{th}$ of the maximum RWA torque.

II. Reaction Wheel Failures

On 25 November 2001, the yaw RWA suffered dramatically increased drag and ceased spinning, but science operations continued with the redundant skew RWA controlling yaw. On 10 December 2001, the pitch RWA also suffered a similar failure, leaving the spacecraft with only two axes of control. The ACS was reconfigured to use the remaining RWAs to stabilize the spacecraft in pitch and roll, but science operations were impossible, due to an uncontrolled tumble in yaw. Efforts to re-start both the yaw and pitch RWAs have resulted in no detectable motion.

After the yaw wheel failure in November 2001, while still operating in three-wheel mode, preliminary investigations began into the feasibility of using the MTBs to generate control torque. Geomagnetic torque has been used in conjunction with spin-stabilization for quite some time[3], but this approach is clearly incompatible with the existing design and three-axis control requirements of FUSE. It has also been suggested as a method of control for satellites whose design provides inherent gravity gradient stabilization[4], but science demands require that FUSE observe targets all over the sky and hold attitudes that do not minimize gravity gradient torque. At any rate, purely magnetic pointing control has only been applied to missions where the tolerances for attitude control were at the 1º level[5]. Since torque can never be generated about the instantaneous geomagnetic field vector, any mission that uses magnetic control torques must have additional actuators, or accept attitude disturbances about a vector that is moving relative to inertial space.

In the case of FUSE, the actuators are the two remaining reaction wheels. Initial calculations showed that the MTBs could be commanded with sufficiently high bandwidth for fine pointing control within the science requirements, and that they could produce enough torque to cancel external disturbances, but only at *some* spacecraft orientations. After the second permanent RWA failure, simultaneous efforts began to upgrade the ACS software to accomplish magnetic control, and to develop ground-based models useful for predicting stable spacecraft orientations. This development, as well as other unrelated ACS modifications, has also been summarized in Ref. 6.

III. Attitude Control System Upgrades

On 24 January 2002, upgraded ACS flight software was installed, and has been incrementally optimized over the two following years. The most notable changes are described below.

A. Coordinate system change

A new orthogonal coordinate system was adopted, with a "symmetric" axis $\hat{S} = (\hat{X} + \hat{Y})/\sqrt{2}$ and an "anti-symmetric" or "magnetic" axis $\hat{A} = (-\hat{X} + \hat{Y})/\sqrt{2}$. The Z-axis remains the same, aligned with the still-functioning roll reaction wheel. The new S-axis is the projection of the skew RWA axis onto the XY plane; the A-axis, which must be totally controlled with magnetic torque, is orthogonal to both S and Z. This new "SAZ" coordinate frame thus completely decouples wheel and magnetic control torques from each other.

B. Control torque generated by MTBs

The wheel momentum unloading algorithm was modified to calculate *separate* MTB dipole moment commands for unloading and control. Given a geomagnetic field vector rotated into the SAZ body frame, $[B_S \quad B_A \quad B_z]^T$, the basis vector

$$\hat{e}_2 = [-B_z \quad 0 \quad B_s]^T \Big/ \left\| [-B_z \quad 0 \quad B_s]^T \right\| \tag{3}$$

is perpendicular to the A-axis and nearly perpendicular to the instantaneous B field. Torques exerted about this direction will act to unload excess wheel momentum without generating torque about the A-axis. A second basis vector,

$$\hat{e}_1 = \hat{e}_2 \times \vec{B} \Big/ \left\| \hat{e}_2 \times \vec{B} \right\| \tag{4}$$

is orthogonal to both $\vec{B}$ and the unloading basis vector, so torques about this direction affect control over the A-axis.

Using these basis vectors, dipole moment commands for pointing control and unloading are

$$\vec{\mu}_{control} \propto N_{A-axis}\left(\hat{e}_1 \times \vec{B}\right) \text{and } \vec{\mu}_{unload} \propto \Delta H\left(\hat{e}_2 \times \vec{B}\right) \tag{5}$$

where N_{A-axis} is the A-axis component of control torque requested by the ACS, and ΔH is a scaling factor derived from the difference between the remaining RWAs momentum and their commanded momentum bias.

C. Increasing MTB bandwidth

The ACS hardware can only control the torquer bars on or off and uses pulse width modulation (PWM) to generate a time-averaged dipole moment vector that approximates that requested by the unloading and control algorithm. The PWM cycle was reduced from 10 to 3 seconds in order to increase the bandwidth of the A-axis torque command, and thus reduce pointing jitter.

D. Prioritizing control over unloading

Each of the three MTBs has a ~140 Am^2 dipole moment, and the direct addition of the desired control and unloading dipole commands can exceed this saturation value. In this case, the final dipole moment vector has a different direction than desired, and optimal A-axis torque will not be realized. To prevent this, control dipole is decoupled from and prioritized over the unloading dipole by adding a linear combination of unload-only and control-only dipoles by use of Eq. (5),

$$\vec{\mu}_{MTB} = \vec{\mu}_{control} + k\vec{\mu}_{unload}, \text{ with } 0 \le k \le 1, \text{ such that } \left|\mu_{x,y,z}\right| \le 140 \text{ Am}^2 \tag{6}$$

where $\vec{\mu}_{MTB}$ is the final dipole moment command that is to be realized by the MTBs.

E. Minimization of high-frequency control components

In Eq. (6), a saturated $\vec{\mu}_{control}$ guarantees that k=0, in which case there will be no momentum unloading. If this condition exists long enough in a non-conservative gravity gradient environment, the RWA momenta will grow unacceptably high. The ACS was modified to use a low bandwidth controller at times when fine pointing control was not required. This prevents oscillation between positive and negative MTB-saturating dipole moment commands, which effectively blocks wheel momentum unloading.

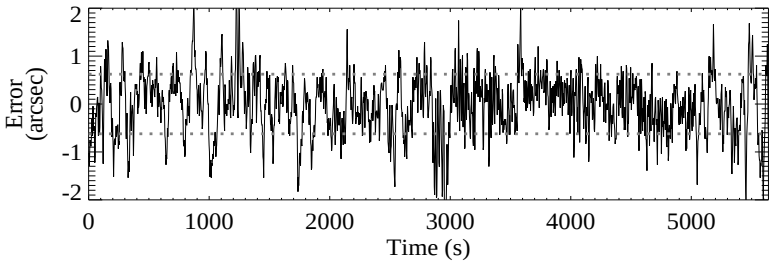

Figure 1. Measured A-axis attitude error during a one orbit span of fine-pointing control. Gray lines indicate ±0.75" RMS jitter (1σ).

Within minutes of the activation of magnetic torque control, three-axis control was regained. Figure 1 shows typical measured attitude error on the A-axis. The RMS pointing jitter of ~0.75" (1σ), as indicated by the dashed gray lines in Fig. 1, is still too small to measurably affect the science data.

IV. Predictive Techniques

The ACS reacts to A-axis disturbances by generating MTB commands as described above, but the available torque is limited and may not be sufficient to maintain pointing control for an arbitrary attitude at a given time. Ground-based predictions must therefore be used to constrain science operations so that observations are scheduled at spacecraft orientations where sufficient torque can be generated to maintain fine pointing control during science exposures, and so that maneuvers can follow their planned trajectory. The important aspects of these predictive techniques are described below.

A. Static Pointing

Even when the spacecraft holds a fixed attitude, the gravity gradient torque and geomagnetic field vectors change their direction and magnitude during the course of one orbit. No magnetic control torque can be generated when $\vec{B}$ is parallel to the A-axis; when the field strength drops, the maximum magnetic torque becomes proportionally smaller. Accounting for all these effects mathematically, the ACS can maintain fine control of the A-axis only when the relation

$$\sum N_A = \left[\vec{N}_{gg} + (\vec{\mu}_{MTB} \times \vec{B})\right] \cdot \hat{\mathrm{A}} = 0 \tag{7}$$

is satisfied. Checking that this relation will hold for a given attitude over a period of time, using an orbit propagator and magnetic field model to predict $\vec{N}_{gg}$ and $\vec{B}$, is now a fundamental planning constraint as science observations are scheduled. In practice, it is computationally feasible to check for the satisfaction of Eq. (7) in 60 second time steps for all targets available for planning. Equation 7 can be adapted to show the absolute margin of excess *torque authority* available at any instant. Given a hypothetical torque command that fully saturates all torquer bars and results in a spacecraft dipole moment $\vec{\mu}_{\max}$, then,

$$N_{\text{margin}} = \left|\left(\vec{\mu}_{\max} \times \vec{B}\right) \cdot \hat{\mathrm{A}}\right| - \left|\hat{N}_{gg} \cdot \hat{\mathrm{A}}\right| \tag{8}$$

In Fig. 2, the gray shaded region graphically depicts the maximum torque "envelope" during an orbit-long dwell at an attitude where the A-axis gravity gradient disturbance torques are consistently less than the maximum A-axis torque authority. At this attitude, Eq. 8 would yield positive values throughout, and the ACS will be able to maintain arcsecond level fine pointing control.

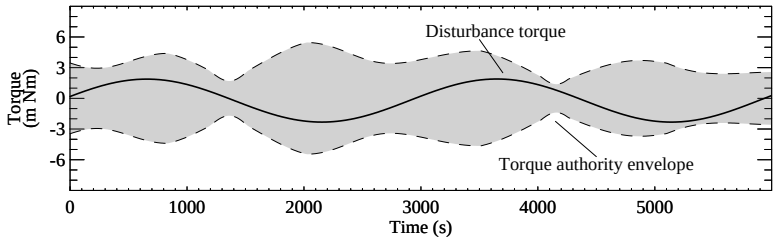

Figure 2. A-axis torque authority envelope at a stable orientation.

Figure 3 shows a one-orbit simulation over the *same timespan*, but at a different spacecraft attitude where the disturbance torques are at times greater than the maximum torque authority. Even though the ECI geomagnetic field vectors are identical in the simulations shown in Fig. 2 and Fig. 3, the torque authority envelope in Fig. 3 is more restricted, because this particular spacecraft attitude has resulted in a less favorable magnetic field vector alignment with the MTBs. Additionally, the component of gravity gradient disturbance on the A-axis is larger at the orientation in Fig. 3 than in Fig. 2.

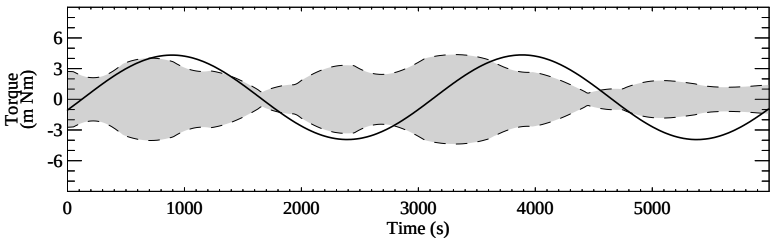

Figure 3. A-axis torque authority envelope at an unstable orientation.

The satellite's yaw and pitch are determined by the celestial coordinates of the target being observed, but in most observation scenarios, *roll* about the instrument boresight can be adjusted through a range of 35˚, while staying within power and thermal constraints. This free parameter can often be used to improve the relative alignment of gravity gradient and B-field vectors and thereby increase the duration of positive torque authority.

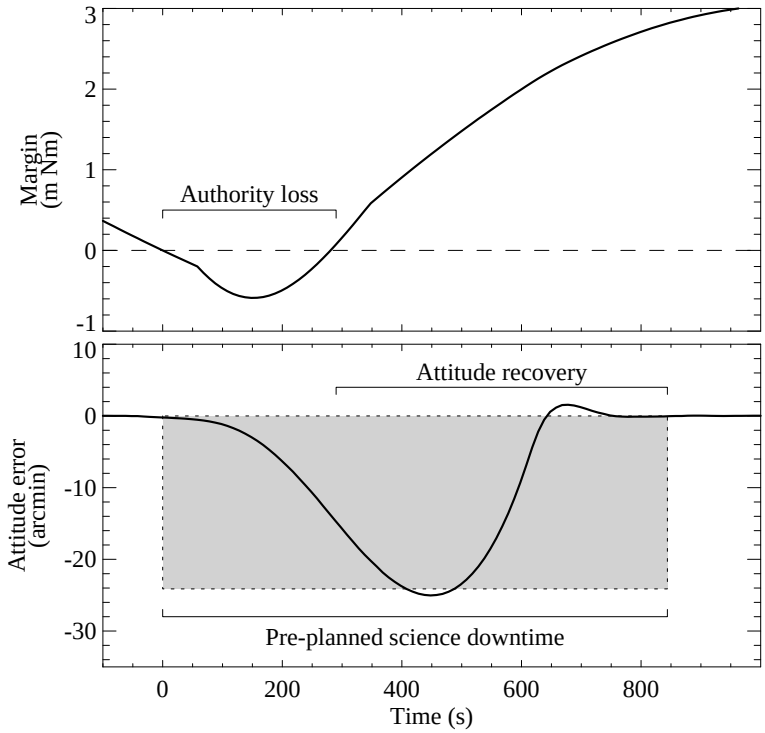

Figure 4. A predicted loss of torque authority.

The most conservative approach would be to schedule observations only at times and attitudes when they are predicted to have positive torque authority throughout the duration of the visit. Since FUSE is in low-earth orbit, the earth often blocks the telescope boresight during a fraction of each orbit, at which time science exposures are halted. During these periods, modest (<5˚) attitude errors have no impact on scheduling efficiency or satellite health and safety, and can be allowed as long as they have been cancelled out by the time the science target becomes visible again. Small (<0.5º) attitude errors are even acceptable during periods of target visibility, as long as the errors can be predicted during planning, and science exposures can be halted and resumed at the appropriate times. Although losses of torque authority in visibility do reduce science efficiency, they often yield a dramatic increase in scheduling flexibility.

Once the start and end times of the loss of torque authority, t_0 and t_1, have been identified by repeated examination of Eq. (7), the attitude angular error that results can be found by integration of the negative torque margin,

$$\begin{aligned} \alpha_{error} &= I^{-1}\left(\left|\left(\vec{\mu}_{\max}\times\vec{B}\right)\cdot\hat{\mathrm{A}}\right| - \left|\hat{N}_{gg}\cdot\hat{\mathrm{A}}\right|\right) \\ \omega_{error} &= \int_{t0}^{t1}\alpha_{error}(t)dt \\ \theta_{error} &= \int_{t0}^{t1}\omega_{error}(t)dt \end{aligned} \tag{9}$$

where I^1 is the inverse of the spacecraft inertia tensor. Although the time required to correct a given attitude error could also be found analytically, in practice an empirical model relating θ_{error} from Eq. (9) to recovery time has proven suitably accurate. Figure 4 shows an example of a small (24 arcmin) angular error resulting from a short loss of torque authority during a period of target visibility. The upper panel of the plot shows predicted torque authority, as defined by Eq. 8, which is negative for approximately 300 seconds. The shaded gray box in the lower panel indicates the *predicted* duration (represented by the box's width) and angular error magnitude (represented by the box's height) resulting from the loss of torque authority. The solid line in the lower panel shows *actual measured* angular error. Since science exposures were halted just before the start of the loss of torque authority, and were resumed approximately 850 seconds later, this predicted loss of torque authority had no effect on science collection.

B. Maneuvers

The ACS must still cancel gravity gradient torques during maneuvers, but additional torque is needed to accelerate and decelerate the spacecraft body and cancel gyroscopic torques. Consequently, it is not necessarily true that a slew will have sufficient torque authority, even if the maneuver is between two stable spacecraft orientations.

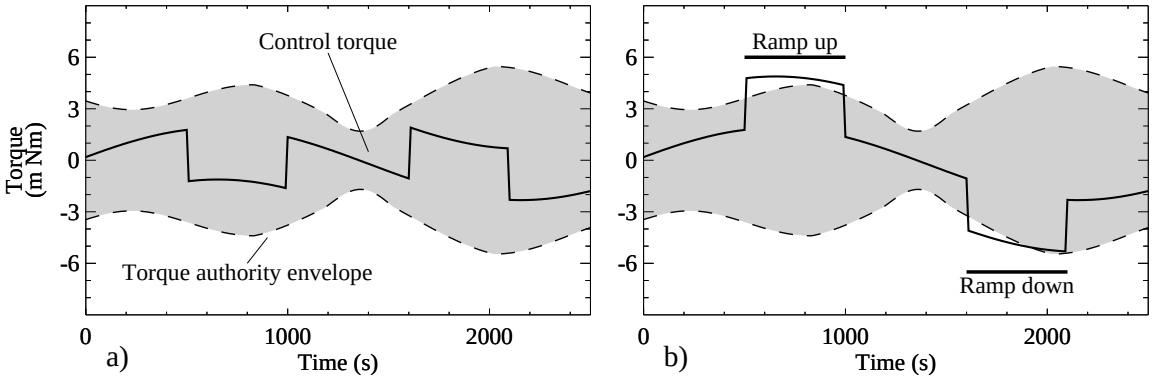

Figure 5. Torque authority envelopes during slews. a) stable maneuver, b) unstable maneuver.

Figure 5a shows the A-axis control torque of a slew that has been timed to phase the ramp-up's negative A-axis acceleration torque with a positive local maximum in A-axis gravity gradient, and has a similar beneficial phasing during the rampdown stage of the slew. At all times, the MTBs are able to generate enough A-axis torque for the slew to follow the ideal trajectory. Figure 5b shows an improperly phased slew in which the total A-axis torque request exceeds torque authority, both during acceleration and deceleration. During the ramp up, the A-axis' position will lag the optimal path, and during ramp-down, the A-axis will overshoot.

FUSE Mission Planning tools simulate each slew as it is scheduled, and choose an optimized start time that guarantees the maximum torque margin throughout. In practice, even 180º slews are usually completed with little or no A-axis pointing errors during the course of the maneuver.

V. Sky Coverage

Equation 7 can be applied to a single spacecraft orientation over a range of times in order to identify windows of stability in which an observation may be scheduled. The same equation can also be applied to range of sky positions, each of which implies a specific spacecraft orientation. The Aitoff projection all-sky maps in Fig. 6 show in black the locus of instrument pointings that will have a net positive torque margin on the A-axis; in white regions, there is insufficient torque authority to keep the spacecraft stable. Figure 6a shows stable regions of the sky at one instant, and 6b shows stable regions at another instant, 40 minutes later. Clearly, regions of stability change dramatically as the gravity gradient and geomagnetic field vectors change. Figure 6c shows in black only regions of the sky that will have continuous positive torque authority throughout an *entire* 100 minute-long orbit.

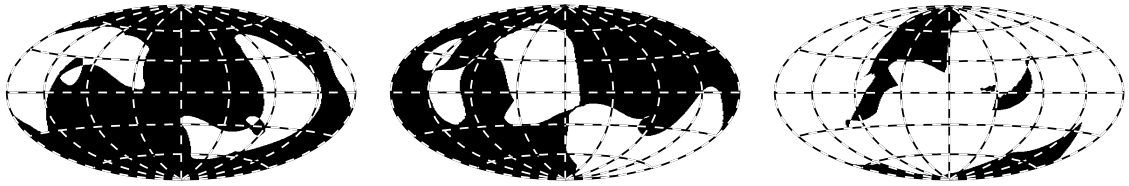

a) **b)** **c)**

Figure 6. Aitoff projection of sky regions with positive torque authority (black) and insufficient torque authority (white). a) At an instant in time, b) at another instant in time 40 minutes later, c) positive torque authority continuously over one 100 minute-long orbit.

The constraint of maintaining positive torque authority throughout an observation must be taken in combination with other mission planning constraints such as lunar, solar and boresight-to-ram direction avoidance. The union of *all* these constraints leaves only small regions of sky availability on any given day, but over time these regions cover different parts of the celestial sphere, thanks to regression of the orbit plane and motion of the earth about the sun. The total sky availability, shown in Fig. 7, illustrates that, while some regions have less time available for scheduling than others, targets at any point in the sky can be scheduled at some point during a calendar year.

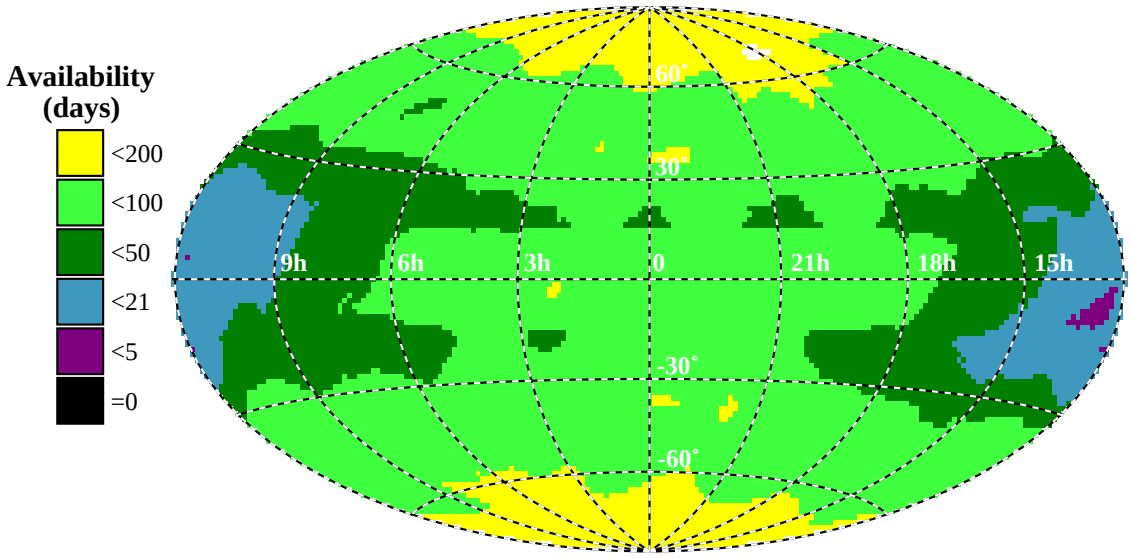

Figure 7. Cumulative sky availability over one year.

VI. Conclusion

Modifications to the FUSE attitude control system and mission planning software have allowed the continuation of an efficient and productive campaign of science observations after the failure of two reaction wheels. While the new control scheme allows less flexibility in scheduling than was enjoyed prior to the wheel failures, the entire sky is available for science observations, and fine pointing jitter is nearly as low as before. Since recovering three-axis control in January 2002, FUSE has conducted over 2500 science observations.

Acknowledgments

The authors acknowledge the support of the FUSE Operations and Science teams, and thank the staff at Orbital Sciences Corporation for assistance in the development efforts described in this paper. The FUSE project at Johns Hopkins University is funded by NASA contract NAS5-32985.

References

1. Moos, H. W., et. al., “Overview of the Far Ultraviolet Spectroscopic Explorer Mission”, *Astrophysical Journal*, Vol. 538, 2000, L1-L6.

2. Sahnow, D. J., et. al., "On-Orbit Performance of the Far Ultraviolet Spectroscopic Explorer Satellite", *Astrophysical Journal*, Vol. 538, 2000, L7-L11.

3. Wertz, J. (ed) Spacecraft Attitude Determination and Control, Kluwer Academic Publishers, Norwell, MA, 2000, pp. 636-642.

4. Arduini, C., and Baiocco, P., “Active Magnetic Damping Attitude Control for Gravity Gradient Stabilized Spacecraft”, *Journal of Guidance, Control and Dynamics*, Vol. 20, No. 1, 1997, pp. 117-122.

5. Wiśniewski, R., “Linear Time-Varying Approach to Satellite Attitude Control Using Only Electromagnetic Actuation”, *Journal of Guidance, Control and Dynamics*, Vol. 23, No. 4, 2000, pp. 640-647.

6. Kruk, J.W., Class, B.F., Rovner, D. and Westphal, J., Ake, T.B., Moos, H.W. and Roberts, B., & Fisher, L. “FUSE In-orbit Attitude Control with Two Reaction Wheels and No Gyroscopes”. *Proc SPIE*, 4854, 2002, 2.